Micromechanical Modeling Of The Finite Deformation Of Thermoelastic Multiphase Composites

Jacob Aboudi
Faculty of Engineering
Tel-Aviv University
Ramat-Aviv 69978, Israel

Steven M. Arnold
Life Prediction Branch
NASA-Lewis Research Center
Cleveland, Ohio 44135, USA

Abstract

A micromechanical model is proposed for the prediction of nonlinearly thermoelastic, multiphase particulate and/or continuous reinforced composites in which any or all constituents exhibit large strain (finite deformation). The analysis provides closed-form representations for the instantaneous mechanical and thermal concentration tensors as well as the effective tangent mechanical and thermal properties of the composite. The micromechanical model predictions are assessed by a comparison with an analytical spherical composite model, valid for hydrostatic loadings only. Very good agreement between the two approaches were obtained. Similarly, results demonstrating the effects of nonlinearity are given for particulate and continuous fiber reinforced S_iC/Al composites. Finally, the nonlinear response of cellular solids idealized by open-cell and closed-cell structures are compared and contrasted.

1 Introduction

The micromechanical prediction of the overall behavior of nonlinearly elastic composites from the knowledge of the properties of the phases which exhibit finite deformation is complicated due to the need to analyze the nonlinear behavior of the materials involved. For nonlinearly elastic composites, results for the overall bulk modulus were given by Ogden(1974) for the case of initially spherical inclusions, dilutely suspended in the matrix, in such a way that there is no mutual interaction between the spheres. Chen and Jiang(1993) considered the problem of finding the second order constants of a particulate composite by using a perturbation approach. More recently, Imam et al.(1995) determined the overall second order constants of an incompressible matrix containing

a dilute concentration of incompressible spherical particles. It should be mentioned that using variational principles, estimates and bounds for the overall properties of certain classes of nonlinear composites have been found by Willis(1990), Talbot and Willis (1987) and Ponte Castaneda and Willis(1988) for example.

The method of cells and its generalization, referred to as the generalized method of cells (**GMC**), is a micromechanical model which is capable of predicting the overall behavior of continuous and discontinuous (particulate) fiber reinforced composites given a knowledge of the properties of the individual phases. A review of the original method of cells was given by Aboudi(1989). More recently this review has been updated by Aboudi (1996), wherein critical assessments of the method, its generalization, and its application by various researchers are outlined.

In the framework of the method of cells, the prediction of nonlinearly elastic composites was presented by Aboudi (1986). In particular, the overall behavior of a foam rubber consisting of a continuum rubber matrix with voids was determined and contrasted with the measurements of Blatz and Ko (1962). The incremental analysis utilized by Aboudi in 1986 was based on a secant approach and required one to solve at every increment a system of **nonlinear** equations.

In this paper we propose, in the framework of the **GMC**, a multiphased micromechanical analysis procedure based on a tangent approach, wherein each and every constituent can be a nonlinear thermoelastic material exhibiting finite deformation. As a result of the tangent approach, and in contrast to the previous secant approach, here one need only solve in each increment a system of linear algebraic equations. Furthermore, in the course of the micromechanical analyses, the instantaneous mechanical concentration tensor (which relates the local deformation gradient to the global one) and effective mechanical tangent tensor (which relates the average stress increment to the average deformation gradient increment), as well as, the instantaneous thermal concentration tensor (which relates the local deformation to the applied temperature deviation) and effective tangent thermal tensor (which relates the average stress increment to the applied temperature deviation) are all established. Note, both the concentration and tangent tensors are given in a closed-form manner in terms of the geometrical dimensions and material properties. It should be emphasized that these instantaneous mechanical and thermal concentration and effective tangent tensors **cannot** be established when the aforementioned secant approach is followed. Furthermore, the establishment of the instantaneous concentration tensors is simply based on a solution of a system of linear algebraic equations.

The validity of the proposed nonlinearly elastic **GMC** prediction is assessed by comparison with

the response of porous materials obtained from an analytical spherical model (whose prediction is valid for hydrostatic loading only). This comparison is performed given three different classes of nonlinearly compressible elastic materials, two of which are known as the harmonic material and the generalized Varga material (Horgan, 1995). Good agreement between the analytical spherical model and **GMC** are shown for all three classes of materials given various amounts of porosities. Similarly, the response of nonlinearly elastic particulate and continuous fiber reinforced S_iC/Al composites are calculated. These results clearly exhibit the existing effects of the nonlinearity of the phases and strongly suggest the need for developing such a finite deformation micromechanics model, particularly when one is interested in predicting the failure of such composite systems. Finally the capability of **GMC** to predict the nonlinear response of opened- and closed-cell cellular solids is illustrated.

2 Material Representation

The micromechanical modeling of a nonlinear thermoelastic composite is based on the knowledge of the current stress tensor and temperature of the constituent materials as well as their tangent tensors at the current state of deformation. For an isotropic thermoelastic nonlinear compressible material, the internal energy is given in terms of the invariants of the Cauchy-Green deformation tensor $\mathbf{C}$ and the entropy s. Thus the internal energy per unit mass of the material can be represented in terms of the three invariants I_1, I_2, and I_3 of the Cauchy-Green deformation tensor, and entropy s in the form:

$$W = W(I_1, I_2, I_3, s) \tag{1}$$

Let $\mathbf{F}$ denote the deformation gradient. The Cauchy-Green deformation tensor $\mathbf{C}$ is given by

$$\mathbf{C} = \mathbf{F}^T\mathbf{F} \tag{2}$$

where the superscript T denotes the transpose operation, and the invariants of $\mathbf{C}$ are

$$\left.\begin{array}{lcll} I_1 & = & \text{tr } \mathbf{C} & = C_{ii} \\ I_2 & = & \frac{1}{2}(\text{ tr}^2\ \mathbf{C} - \text{ tr } \mathbf{C}^2) & = \frac{1}{2}(C_{ii}^2 - C_{ij}C_{ji}) \\ I_3 & = & \det \mathbf{C} & = \frac{1}{6}(C_{ii}^3 - 3C_{ii}C_{ij}C_{ji} + 2C_{ij}C_{jk}C_{ki}) \end{array}\right\} \tag{3}$$

It should be noted that in this paper, the summation convention is implied for repeating Latin indices.

Let us denote by **S** the 2nd (symmetric) Piola-Kirchhoff tensor. It follows that (e.g. Bland, 1969)

$$S_{ij} = \rho_0 \left(\frac{\partial W}{\partial C_{ij}} + \frac{\partial W}{\partial C_{ji}} \right) \tag{4}$$

where ρ_0 is the initial density of the material. Furthermore,

$$S_{ij} = 2\rho_0 \frac{\partial W}{\partial I_p} \frac{\partial I_p}{\partial C_{ij}} \tag{5}$$

where

$$\left.\begin{aligned} \frac{\partial I_1}{\partial C_{ij}} &= \delta_{ij} \\ \frac{\partial I_2}{\partial C_{ij}} &= I_1 \delta_{ij} - C_{ij} \\ \frac{\partial I_3}{\partial C_{ij}} &= I_2 \delta_{ij} - I_1 C_{ij} + C_{ik} C_{kj} \end{aligned}\right\}$$

with δ_{ij} being the Kronecker delta. Thus, the requested expression of **S** for a given material can be readily determined for a given state of deformation.

The temperature, θ, is given in terms of the entropy per unit mass, s, by

$$\theta = \frac{\partial W}{\partial s} \tag{6}$$

With the help of this last equation, one can eliminate the entropy, s, by expressing it in terms of the temperature, θ. This provides a new specific internal energy function $W = W(I_1, I_2, I_3, \theta)$.

Now let us represent the constitutive law of the nonlinearly thermoelastic material in the incremental form:

$$\Delta \mathbf{S} = \frac{1}{2} \mathbf{D} \Delta \mathbf{C} - \boldsymbol{\Gamma} \Delta \theta \tag{7}$$

where **D** and $\boldsymbol{\Gamma}$ denote the instantaneous mechanical and thermal tangent tensors, respectively.

The tangent tensor, **D**, of the material at the current instant of loading is determined from

$$D_{ijkl} = \frac{\partial S_{ij}}{\partial C_{kl}} + \frac{\partial S_{ij}}{\partial C_{lk}} = 4\rho_0 \frac{\partial^2 W}{\partial C_{ij} \partial C_{kl}} \tag{8}$$

In establishing the requested tangent modulus **D** for a given material, the following relations have to be used:

$$\begin{aligned} \frac{\partial^2 I_1}{\partial C_{ij} \partial C_{kl}} &= 0 \\ \frac{\partial^2 I_2}{\partial C_{ij} \partial C_{kl}} &= \delta_{ij}\delta_{kl} - I^{(4)}_{ijkl} \\ \frac{\partial^2 I_3}{\partial C_{ij} \partial C_{kl}} &= (I_1 \delta_{kl} - C_{kl})\delta_{ij} - C_{ij}\delta_{kl} - I_1 I^{(4)}_{ijkl} \end{aligned}$$

$$+ \quad \frac{1}{2}(\delta_{ik}C_{jl} + \delta_{il}C_{jk})$$
$$+ \quad \frac{1}{2}(C_{ik}\delta_{jl} + C_{il}\delta_{jk}) \tag{9}$$

and

$$I^{(4)}_{ijkl} = \frac{1}{2}(\delta_{ik}\ \delta_{jl} + \delta_{il}\ \delta_{jk})$$

The current thermal tangent tensor $\mathbf{\Gamma}$ is determined from

$$\Gamma_{ij} = -\frac{\partial S_{ij}}{\partial \theta} = -\rho_0\left(\frac{\partial^2 W}{\partial C_{ij}\partial\theta} + \frac{\partial^2 W}{\partial C_{ji}\partial\theta}\right) \tag{10}$$

Five examples taken from the literature for representing the isotropic internal strain energy (W) in terms of the above three strain invariants (I_1, I_2, and I_3) and temperature (θ) are given in Table 1. Four of the five models are defined as isothermal representations, whereas one is a nonisothermal model. Clearly, the current tangent moduli $\mathbf{D}$ and $\mathbf{\Gamma}$ can be readily determined given the functional form of the strain energy by using eqn.(8) and (10).

Table1:Various representations for nonlinear elastic material behavior

Model (reference)	Strain Energy ($\rho_0 W$)	Material Constants
Blatz and Ko (1962)	$\frac{\mu}{2}(\frac{I_2}{I_3} + 2\ I_3^{1/2} - 5)$	μ
Murnaghan (1967)	$\frac{\lambda+2\mu}{2}\ K_1^2 - 2\mu\ K_2 + \frac{l+2m}{3}\ K_1^3$ $-2m\ K_1K_2 + n\ K_3$	λ, μ, l, m, n
Blatz (1969)	$\frac{K}{k}[I_3^{1/2} - \frac{k}{k-1} + \frac{I_3^{(1-k)/2}}{k-1}] + \frac{\mu}{2}[I_1 - 3I_3^{1/3}]$	μ, K, k
St. Venant-Kirchhoff (Bland, 1969)	$\frac{\lambda+2\mu}{2}K_1^2 - 2\mu K_2 + \frac{\rho_0}{2\eta}[\theta^2 - (\theta_0 - \kappa K_1)^2]$	θ_0 , λ, μ, κ, and η
Mooney-Rivlin (Sussman and Bathe, 1987)	$C_1(J_1 - 3) + C_2(J_2 - 3) + \frac{\kappa}{2}(J_3 - 1)^2$	C_1, C_2, and κ
where other invariants are	$J_1 = I_1/I_3^{1/3}$ $\quad K_1 = \frac{1}{2}(I_1 - 3)$ $J_2 = I_2/I_3^{2/3}$ $\quad K_2 = \frac{1}{4}(-2I_1 + I_2 + 3)$ $J_3 = I_3^{1/2}$ $\quad K_3 = \frac{1}{2}(I_1 - I_2 + I_3 - 1)$	

Finally, as the micromechanical analysis described in the following section utilizes the first Piola-Kirchhoff stress tensor $\mathbf{T}$, instead of the second, we need to relate the displacement gradient

and temperature increments to the corresponding first Piola-Kirchhoff stress increment. To this end, we can use eqn.(2) in order to rewrite eqn. (7), and, after some manipulations obtain the following:

$$\Delta \mathbf{S} = \mathbf{Q}\ \Delta \mathbf{F} - \mathbf{\Gamma} \Delta \boldsymbol{\theta} \tag{11}$$

where

$$Q_{ijkl} = \frac{1}{2}[D_{ijlp}\ F_{kp} + D_{ijpl}\ F_{kp}] \tag{12}$$

Given the fact that the relationship between the first and second Piola-Kirchhoff stresses is defined as

$$\mathbf{T} = \mathbf{S}\ \mathbf{F}^T \tag{13}$$

it follows, then, after some manipulations, that the desired incremental constitutive relation for the considered nonlinear thermoelastic constituent material is:

$$\Delta \mathbf{T} = \mathbf{R}\ \Delta \mathbf{F} - \mathbf{H} \Delta \boldsymbol{\theta} \tag{14}$$

where the current mechanical and thermal **tangent** tensors **R** and **H** are given by

$$R_{ijkl} = Q_{ipkl} F_{jp} + S_{il}\ \delta_{jk} \tag{15}$$

and

$$H_{ij} = \Gamma_{ik} F_{jk} \tag{16}$$

It is readily observed that the determination of **R** at a given state of deformation **F** depends on the knowledge of **S** and **D**. Similarly, the instantaneous tangent thermal tensor **H** depends on the current deformation gradient.

3 Micromechanical Analysis

3.1 Model Description

Consider a multiphase composite material in which some or all phases are modeled as nonlinearly thermoelastic materials. It is assumed that the composite possesses a periodic structure such that a repeating cell can be defined. In Fig. 1, such a repeating cell is shown which consists of $N_\alpha N_\beta N_\gamma$ rectangular parallelepiped subcells. The volume of each subcell is $d_\alpha h_\beta l_\gamma$, where α, β, γ are running

indices $\alpha = 1, \cdots, N_\alpha$; $\beta = 1, \cdots, N_\beta$; $\gamma = 1, \cdots, N_\gamma$ in the three orthogonal directions, respectively. The volume of the repeating cell is dhl where

$$d = \sum_{\alpha=1}^{N_\alpha} d_\alpha \ , \ h = \sum_{\beta=1}^{N_\beta} h_\beta \ , \ l = \sum_{\gamma=1}^{N_\gamma} l_\gamma \tag{17}$$

Any subcell can be filled in general by nonlinearly thermoelastic materials; with nonlinear unidirectional continuous and/or discontinuous fiber reinforced composites, nonlinear porous materials, and laminated materials being obtained by merely a proper selection of the geometrical dimensions of the subcells and appropriate material descriptions.

The following formulation is based on a Lagrangian description of the motion of the composite. To this end, let $\mathbf{X}$ denote the position of a material point in the undeformed configuration at time $t = 0$. The location of this point in the deformed configuration is denoted by $\mathbf{x}$. This current position is given by

$$\mathbf{x} = \mathbf{X} + \mathbf{u}(\mathbf{X}, t) \tag{18}$$

where $\mathbf{u}$ denotes the displacement vector.

The micromechanical model employs a first order expansion of the displacement increment in the subcell $(\alpha\beta\gamma)$ in terms of the local coordinates $(\bar{X}_1^{(\alpha)}, \bar{X}_2^{(\beta)}, \bar{X}_3^{(\gamma)})$ located at the center of the subcell.

$$\Delta\mathbf{u}^{(\alpha\beta\gamma)} = \Delta\mathbf{w}^{(\alpha\beta\gamma)} + \bar{X}_1^{(\alpha)}\Delta\boldsymbol{\phi}^{(\alpha\beta\gamma)} + \bar{X}_2^{(\beta)}\,\Delta\boldsymbol{\chi}^{(\alpha\beta\gamma)} + \bar{X}_2^{(\gamma)}\,\Delta\boldsymbol{\psi}^{(\alpha\beta\gamma)} \tag{19}$$

The increment of the deformation gradient in the subcell is given according to (19) by

$$\Delta\mathbf{F}^{(\alpha\beta\gamma)} = \begin{bmatrix} \Delta\phi_1^{(\alpha\beta\gamma)} & \Delta\chi_1^{(\alpha\beta\gamma)} & \Delta\psi_1^{(\alpha\beta\gamma)} \\ \Delta\phi_2^{(\alpha\beta\gamma)} & \Delta\chi_2^{(\alpha\beta\gamma)} & \Delta\psi_2^{(\alpha\beta\gamma)} \\ \Delta\phi_3^{(\alpha\beta\gamma)} & \Delta\chi_3^{(\alpha\beta\gamma)} & \Delta\psi_3^{(\alpha\beta\gamma)} \end{bmatrix} \tag{20}$$

The average deformation gradient in the entire repeating cell is given by

$$\Delta\bar{\mathbf{F}} = \frac{1}{dhl}\sum_{\alpha=1}^{N_\alpha}\sum_{\beta=1}^{N_\beta}\sum_{\gamma=1}^{N_\gamma} d_\alpha\, h_\beta\, l_\gamma\, \Delta\mathbf{F}^{(\alpha\beta\gamma)} \tag{21}$$

Similarly, let the increment of the first Piola-Kirchhoff stress tensor in subcell $(\alpha\beta\gamma)$ be denoted by $\Delta\mathbf{T}^{(\alpha\beta\gamma)}$. Then the average increment of this stress tensor is given by

$$\Delta\bar{\mathbf{T}} = \frac{1}{dhl}\sum_{\alpha=1}^{N_\alpha}\sum_{\beta=1}^{N_\beta}\sum_{\gamma=1}^{N_\gamma} d_\alpha\, h_\beta\, l_\gamma\, \Delta\mathbf{T}^{(\alpha\beta\gamma)} \tag{22}$$

Given these definitions we can establish, as shown in the next section, closed-form expressions for the instantaneous concentration tensor that relates the increment of the deformation gradient $\Delta\mathbf{F}^{(\alpha\beta\gamma)}$ in the subcell $(\alpha\beta\gamma)$, to the average (or global) increment of the deformation gradient $\Delta\bar{\mathbf{F}}$. Similarly, closed-form expression are established for the instantaneous thermal tensor that relates the subcell's deformation gradient increment to the temperature increment. The derivation of such relationships that link the local and global quantities is referred to as localization. The subsequent use of these localization relationships can establish a relationship between the increment of the global stress tensor $\Delta\bar{\mathbf{T}}$ and the increments of the global deformation gradient $\Delta\bar{\mathbf{F}}$ and temperature, θ.

3.2 Interfacial Continuity of Displacement Increments

The development of the composite constitutive relationships are based on the satisfaction of equilibrium within the subcell, and the fulfillment of the continuity of displacement and tractions at the interfaces between the subcells in the repeating cells, and between neighboring cells. The establishment of these relations in the present case of finite deformations is similar to that described previously in the case of infinitesimal deformation (Aboudi, 1995). For a detailed explanation of the two-dimensional infinitesimal case with 2 by 2 subcells see a recent book by Herakovich (1997).

For finite deformation, the conditions of continuity of displacement increments at the various interfaces provide the following relations between the average deformation gradient increments and the subcells deformation gradient increments.

$$\sum_{\alpha=1}^{N_\alpha} d_\alpha \, \Delta F_{i1}^{(\alpha\beta\gamma)} = d \, \Delta\bar{F}_{i1} \qquad i=1,2,3 \;\; ; \;\; \beta=1,\cdots,N_\beta \;\; ; \;\; \gamma=1,\cdots,N_\gamma \tag{23}$$

$$\sum_{\beta=1}^{N_\beta} h_\beta \, \Delta F_{i2}^{(\alpha\beta\gamma)} = h \, \Delta\bar{F}_{i2} \qquad i=1,2,3 \;\; ; \;\; \alpha=1,\cdots,N_\alpha \;\; ; \;\; \gamma=1,\cdots,N_\gamma \tag{24}$$

$$\sum_{\gamma=1}^{N_\gamma} l_\gamma \, \Delta F_{i3}^{(\alpha\beta\gamma)} = l \, \Delta\bar{F}_{i3} \qquad i=1,2,3 \;\; ; \;\; \alpha=1,\cdots,N_\alpha \;\; ; \;\; \beta=1,\cdots,N_\beta \tag{25}$$

and

$$\Delta\bar{F}_{ij} = \Delta\frac{\partial w_i}{\partial X_j} \qquad i,j=1,2,3 \tag{26}$$

with

$$\frac{\partial w_i^{(\alpha\beta\gamma)}}{\partial X_j} = \frac{\partial w_i}{\partial X_j} \tag{27}$$

Equations (23)-(25) form a set of $3(N_\alpha N_\beta + N_\alpha N_\gamma + N_\beta N_\gamma)$ relations, and can be written in a compact matrix form as follows

$$\mathbf{A}_G \; \Delta \mathbf{F}_s = \mathbf{J} \; \Delta \bar{\mathbf{F}} \tag{28}$$

where $\Delta \mathbf{F}_s$ contains the increments of the deformation gradients of all subcells as follows

$$\Delta \mathbf{F}_s = [\Delta \mathbf{F}^{(111)}, \cdots, \Delta \mathbf{F}^{(N_\alpha N_\beta N_\gamma)}] \tag{29}$$

and $\Delta \mathbf{F}^{(\alpha\beta\gamma)}$ are the appropriate matrices. It should be noted that the matrix $\mathbf{A_G}$ (whose order is $3(N_\alpha N_\beta + N_\alpha N_\gamma + N_\alpha N_\gamma)$ by $9N_\alpha N_\beta N_\gamma$) involves the geometrical dimensions of the subcells within the repeating cell only. The $3(N_\alpha N_\beta + N_\alpha N_\gamma + N_\alpha N_\gamma)$ by 9 matrix $\mathbf{J}$ involves the geometrical dimensions of the cell.

3.3 Interfacial Continuity of Traction Increments

From the continuity of the traction increments at the interfaces of the subcells within a repeating cell, and at the interfaces between neighboring cells we have

$$\Delta T_{1i}^{(\alpha\beta\gamma)} = \Delta T_{1i}^{(\hat{\alpha}\beta\gamma)} \quad \alpha = 1, \cdots, N_\alpha - 1 \; ; \; \beta = 1, \cdots, N_\beta \; ; \; \gamma = 1, \cdots, N_\gamma \tag{30}$$

$$\Delta T_{2i}^{(\alpha\beta\gamma)} = \Delta T_{2i}^{(\alpha\hat{\beta}\gamma)} \quad \alpha = 1, \cdots, N_\alpha \; ; \; \beta = 1, \cdots, N_\beta - 1 \; ; \; \gamma = 1, \cdots, N_\gamma \tag{31}$$

$$\Delta T_{3i}^{(\alpha\beta\gamma)} = \Delta T_{3i}^{(\alpha\beta\hat{\gamma})} \quad \alpha = 1, \cdots, N_\alpha \; ; \; \beta = 1, \cdots, N_\beta \; ; \; \gamma = 1, \cdots, N_\gamma - 1 \tag{32}$$

with $i = 1, 2, 3$. In these equations $\hat{\alpha}, \hat{\beta}, \hat{\gamma}$ are defined as follows

$$\hat{\alpha} = \begin{cases} \alpha + 1 & \alpha < N_\alpha \\ 1 & \alpha = N_\alpha \end{cases}$$

$$\hat{\beta} = \begin{cases} \beta + 1 & \beta < N_\beta \\ 1 & \beta = N_\beta \end{cases}$$

$$\hat{\gamma} = \begin{cases} \gamma + 1 & \gamma < N_\gamma \\ 1 & \gamma = N_\gamma \end{cases} \tag{33}$$

These definitions ensure that for an interior subcell α (say) within the repeating cell, the neighboring subcell in the X_1 direction is the one labeled by $\alpha + 1$ within this repeating cell. For $\alpha = N_\alpha$,on the other hand, the neighboring subcell is within the next repeating cell whose first subcell is $\alpha = 1$.

The traction increments in eqns. (30)-(32) are given by eqn (14). Consequently, conditions (30)-(32) provide a set of $9N_\alpha N_\beta N_\gamma - 3(N_\alpha N_\beta + N_\alpha N_\gamma + N_\beta N_\gamma)$ relations between the tangent tensors $\mathbf{R}^{(\alpha\beta\gamma)}$ and $\mathbf{H}^{(\alpha\beta\gamma)}$ of the various subcells. This set can be represented in a compact matrix form as follows

$$\mathbf{A}_M \, \Delta\mathbf{F}_s = \mathbf{G_M} \Delta\boldsymbol{\theta} \tag{34}$$

where the matrix $\mathbf{A}_M$ (whose order is $9N_\alpha N_\beta N_\gamma - 3(N_\alpha N_\beta + N_\alpha N_\gamma + N_\beta N_\gamma)$ by $9N_\alpha N_\beta N_\alpha$) involves the tangent tensors $\mathbf{R}^{(\alpha\beta\gamma)}$ of the material in the subcells, while $\mathbf{G_M}$ is a $9N_\alpha N_\beta N_\gamma - 3(N_\alpha N_\beta + N_\alpha N_\gamma + N_\beta N_\gamma)$ by one matrix that assembles the thermal tensors $\mathbf{H}^{(\alpha\beta\gamma)}$.

3.4 Overall Nonlinear Thermomechanical Constitutive Law

The combination of eqns(34) and (28) leads to the following system of **linear** algebraic equations in the unknown local deformation gradient increments $\Delta\mathbf{F}_s$:

$$\tilde{\mathbf{A}} \, \Delta\mathbf{F}_s = \mathbf{K} \, \Delta\bar{\mathbf{F}} + \tilde{\mathbf{G}} \, \Delta\theta \tag{35}$$

where

$$\tilde{\mathbf{A}} = \begin{bmatrix} \mathbf{A}_M \\ \mathbf{A}_G \end{bmatrix} , \quad \mathbf{K} = \begin{bmatrix} \mathbf{0} \\ \mathbf{J} \end{bmatrix} , \quad \tilde{\mathbf{G}} = \begin{bmatrix} \mathbf{G}_M \\ \mathbf{0} \end{bmatrix}$$

where the order of the square matrix $\tilde{\mathbf{A}}$ is $9N_\alpha N_\beta N_\alpha$.

Solving eqn.(35) yields

$$\Delta\mathbf{F}_s = \mathbf{A} \, \Delta\bar{\mathbf{F}} + \mathbf{G} \, \Delta\boldsymbol{\theta} \tag{36}$$

where

$$\mathbf{A} = \tilde{\mathbf{A}}^{-1} \, \mathbf{K}$$

and

$$\mathbf{G} = \tilde{\mathbf{A}}^{-1} \, \tilde{\mathbf{G}}$$

$\mathbf{A}$ is the requested current mechanical concentration tensor which is represented as a square matrix whose order is $9N_\alpha N_\beta N_\gamma$. Similarly, $\mathbf{G}$ is the current thermal concentration tensor which is represented as $9N_\alpha N_\beta N_\gamma$ vector.

Let the concentration matrix $\mathbf{A}$ be partitioned into $N_\alpha N_\beta N_\gamma$ 9-order square submatrices in the form

$$\mathbf{A} = \begin{bmatrix} \mathbf{A}^{(111)} \\ \vdots \\ \mathbf{A}^{(N_\alpha N_\beta N_\gamma)} \end{bmatrix} \tag{37}$$

Similarly let the thermal concentration vector $\mathbf{G}$ be partitioned as follows

$$\mathbf{G} = \begin{bmatrix} \mathbf{G}^{(111)} \\ \vdots \\ \mathbf{G}^{(N_\alpha N_\beta N_\gamma)} \end{bmatrix} \tag{38}$$

It follows from eqn. (36) that

$$\Delta\mathbf{F}^{(\alpha\beta\gamma)} = \mathbf{A}^{(\alpha\beta\gamma)}\ \Delta\bar{\mathbf{F}} + \mathbf{G}^{(\alpha\beta\gamma)}\Delta\theta \tag{39}$$

Equation (39) expresses the deformation gradient increment in the subcell $(\alpha\beta\gamma)$ in terms of the applied average (macro) deformation gradient and temperature increments, via the mechanical and thermal concentration tensors $\mathbf{A}^{(\alpha\beta\gamma)}$ and $\mathbf{G}^{(\alpha\beta\gamma)}$, respectively.

Substitution of eqn.(39) into relation (14), that governs the nonlinear material behavior in subcell $(\alpha\beta\gamma)$, provides

$$\Delta\bar{\mathbf{T}}^{(\alpha\beta\gamma)} = \mathbf{R}^{(\alpha\beta\gamma)}[\ \mathbf{A}^{(\alpha\beta\gamma)}\ \Delta\bar{\mathbf{F}} +\ \mathbf{G}^{(\alpha\beta\gamma)}\ \Delta\theta\ ] -\ \mathbf{H}^{(\alpha\beta\gamma)}\ \Delta\theta \tag{40}$$

Consequently, in conjunction with eqn.(22), the following overall (macroscopic) nonlinear, anisotropic, thermoelastic constitutive law governing the average behavior of the multiphased composite is established

$$\Delta\bar{\mathbf{T}} = \mathbf{R}^*\ \Delta\bar{\mathbf{F}} - \mathbf{H}^*\Delta\theta \tag{41}$$

where the current effective tangent tensor,$\mathbf{R}^*$, that relates the average first Piola-Kirchhoff increment, $\Delta\bar{\mathbf{T}}$, to the applied average deformation gradient increment, $\Delta\bar{\mathbf{F}}$, is given in a closed-form manner by

$$\mathbf{R}^* = \frac{1}{dhl}\sum_{\alpha=1}^{N_\alpha}\sum_{\beta=1}^{N_\beta}\sum_{\gamma=1}^{N_\gamma} d_\alpha\ h_\beta\ l_\gamma\ \mathbf{R}^{(\alpha\beta\gamma)}\ \mathbf{A}^{(\alpha\beta\gamma)} \tag{42}$$

whereas the current effective thermal tensor, $\mathbf{H}^*$, is given by

$$\mathbf{H}^* = \frac{1}{dhl}\sum_{\alpha=1}^{N_\alpha}\sum_{\beta=1}^{N_\beta}\sum_{\gamma=1}^{N_\gamma} d_\alpha\ h_\beta\ l_\gamma\ [\ \mathbf{R}^{(\alpha\beta\gamma)}\ \mathbf{G}^{(\alpha\beta\gamma)} - \mathbf{H}^{(\alpha\beta\gamma)}\ ] \tag{43}$$

It is comforting to note, as one might expect, that the derived macroscopic effective constitutive law (eq. 41) has an identical form as the constitutive relation for the constituent material given in eq. (14). This is due to the fact that one can construct the macroscopic instantaneous stiffness and thermal tensors ($\mathbf{R}^*$, $\mathbf{H}^*$) in terms of their respective local ones, through the established evolving mechanical and thermal concentration tensors ($\mathbf{A}$ and $\mathbf{G}$).

Once $\mathbf{R}^*$ and $\mathbf{H}^*$ have been determined at the current stage of deformation, one can obtain the current average stress tensor $\bar{\mathbf{T}}$ from the computed stress at the previous stage $\bar{\mathbf{T}}|_{previous}$ according to $\bar{\mathbf{T}} = \bar{\mathbf{T}}|_{previous} + \Delta\bar{\mathbf{T}}$. Similarly, the current local $\mathbf{F}^{(\alpha\beta\gamma)}$ and average $\bar{\mathbf{F}}$ deformation gradients can be determined. Clearly, one must select an appropriately small load increment to ensure convergence of the incremental solution. This increment will depend of course on the severity of the material nonlinearity and the applied loading direction.

The derived constitutive law, eqns.(41), that governs the overall behavior of the nonlinear multiphase thermoelastic composite, has the advantage that it can be readily utilized irrespective of whether loading symmetry exists or not, as well as without resorting to different boundary condition application strategies as in the case of the finite element unit cell procedure. Furthermore, the availability of an analytical expression representing the macro response of the composite is particularly important when analyzing realistic structural components, since different loading conditions exist throughout the structure, thus necessitating the application of the macromechanical equations repeatedly at these locations.

By using eqns.(12) and (15) for the effective tangent tensors, we can readily establish the current effective tangent tensor $\mathbf{D}^*$ that relates the increment of the average of the second Piola-Kirchhoff, $\Delta\bar{\mathbf{S}}$, to the increment of the average Cauchy-Green deformation tensor, $\Delta\bar{\mathbf{C}}$, in the form

$$D^*_{ijkl} = Q^*_{ijpk}\bar{F}^{-1}_{lp} \tag{44}$$

where

$$Q^*_{ijpk} = (R^*_{iqpk} - \delta_{pq}\bar{S}_{ik})\bar{F}^{-1}_{jq}$$

with $\bar{\mathbf{S}} = \bar{\mathbf{T}}\left[\bar{\mathbf{F}}^{\mathbf{T}}\right]^{-1}$ being the average second Piola-Kirchhoff stress tensor, and $\bar{\mathbf{F}}^{-1}$ is the inverse of $\bar{\mathbf{F}}$.

We conclude this section by noting that in the special case of infinitesimal deformations, the present derivation reduces to that given previously by Aboudi (1995). In this special case the material properties are constant for any applied deformation history, consequently the incremental procedure is no longer required since $\mathbf{R}^*$ and $\mathbf{H}^*$ become constants, since the concentration tensors $\mathbf{A}$ and $\mathbf{G}$ no longer evolve.

4 Validation and Results

4.1 Formulation and Constitutive Model Implementation Validation

In order to validate the above derived micromechanical model, one would like to compare its predictive ability with actual experimental data or if none is available than at least with some known analytical solution. To the authors knowledge, the only meaningful analytical comparison that can be performed is with the composite spherical model, see Hashin (1985). Under hydrostatic (isotropic) deformation, this spherical model provides the overall stress-deformation relation of a porous media consisting of a finite-deforming matrix with an arbitrary concentration of spherical voids. In the framework of the composite spherical model, the stress-deformation response of a single hollow sphere subjected to hydrostatic (isotropic) deformation coincides with that of the effective response of the entire composite subjected to the same isotropic loading. It should be noted, however, that the response of composites to other types of loading cannot be modeled by the spherical assemblage representation. For an incompressible nonlinearly elastic matrix of the Mooney-Rivlin type (e.g., see Table 1) with voids, the isotropic deformation of the porous medium was established by Hashin (1985). Here we employ this spherical model and present resulting response for three different classes of **compressible** nonlinearly elastic matrices with voids.

To this end, the isothermal response of a thick-wall spherical shell subjected to isotropic deformation at the outer surface, while keeping the inner surface traction-free, must be determined. The reference geometry of the spherical shell (see Fig. 2a, which depicts for simplicity a half shell) is defined by

$$A \leq R \leq B, \quad 0 \leq \Theta \leq \pi, \quad 0 \leq \Phi \leq 2\pi \tag{45}$$

in terms of spherical polar coordinates (R, Θ, Φ). The current geometry is defined by

$$a \leq r(R) \leq b, \quad \theta = \Theta, \quad \phi = \Phi, \tag{46}$$

in terms of spherical polar coordinates (r, θ, ϕ), and the deformation gradient is given by

$$\mathbf{F} = diag(\frac{dr}{dR}, \frac{r}{R}, \frac{r}{R}) \tag{47}$$

Hence the principal stretches $\lambda_1, \lambda_2, \lambda_3$ corresponding to coordinate directions r, θ, ϕ respectively are

$$\lambda_1 = \frac{dr}{dR}, \quad \lambda_2 = \lambda_3 = \frac{r}{R} \tag{48}$$

Given a strain energy function, $W(\lambda_1, \lambda_2, \lambda_3)$, per unit undeformed volume of an isotropic elastic compressible material, the equation of equilibrium yields a nonlinear second order ordinary differential equation for the unknown function $r(R)$:

$$\frac{d}{dR}(R^2\frac{\partial W}{\partial \lambda_1}) - 2R\frac{\partial W}{\partial \lambda_2} = 0 \tag{49}$$

Closed-form solutions for $r(R)$ (involving two arbitrary constants) resulting from eqn.(49) are obtainable for certain classes of nonlinear compressible materials. These classes of compressible materials have been recently summarized by Horgan (1995).

Once the function $r(R)$ has been obtained for a given type of strain energy W we can proceed, given the spherical model, to establish the response of the nonlinear porous material under hydrostatic loading. This solution is achieved by imposing the following two boundary conditions (which determine the two constants in the closed-form solution) that express the fact that the inner boundary, i.e., $R = A$, is traction-free, whereas at the outer surface (i.e., $R = B$) a uniform deformation is imposed thus at the current configuration $r(B) = b$.

$$\begin{aligned} T_{RR} &= \frac{\partial W}{\partial \lambda_1} = 0, \quad R = A \\ r &= b, \quad R = B \end{aligned} \tag{50}$$

With the function $r(R)$ completely known, we can determine, in particular, the radial stress T_{RR} at the outer surface $R = B$. Hence we conclude from the average stress theorem (e.g., Aboudi(1991)) that the average radial component of the first Piola-Kirchhoff stress tensor in the spherical shell is also given by the same expression $T_{RR}(R = B)$. Consequently, the effective stress - deformation relationship of the porous material has been established when it is subjected to a hydrostatic (isotropic) loading defined by the ratio b/B. The initial volume concentration of the pores is given by $A^3/B^3 < 1$.

In the following, three classes of nonlinearly elastic compressible materials are considered. Following Horgan(1995), these classes are referred to as classes I, II and III and are described in terms of the three invariants i_1, i_2, i_3 of the stretch tensor. These invariants are given in terms of λ_i as follows:

$$\begin{aligned} i_1 &= \lambda_1 + \lambda_2 + \lambda_3 \\ i_2 &= \lambda_1\lambda_2 + \lambda_1\lambda_3 + \lambda_2\lambda_3 \\ i_3 &= \lambda_1\lambda_2\lambda_3 \end{aligned} \tag{51}$$

Note, every class exhibits essentially a different material response as the strain energy within each class has a different invariant functional dependence. By contrasting, for each class, the predicted **GMC** response with that provided by the spherical model, we can assess the reliability of the predicted **GMC** response under the present circumstances, and examine whether **GMC**'s accuracy is affected by various material classes.

4.1.1 Class I - Harmonic Material

Here the strain energy function is described by

$$W = f(i_1) + c_2(i_2 - 3) + c_3(i_3 - 1), \quad f''(i_1) \neq 0 \tag{52}$$

where f is an arbitrary function of the *first* invariant and c_i are material constants. In this case the solution of eqn.(49) is given by

$$r(R) = \xi R + \frac{\eta}{R^2} \tag{53}$$

Then imposing the boundary conditions given in eqns (50), the constants ξ and η can be determined. Hence it is possible, according to the spherical model, to determine the resulting average radial stress field in the porous material when subjected to an isotropic loading profile.

Following Ogden(1984) let us consider the following specific harmonic material:

$$W = \frac{2\nu - \mu}{27} {i_1}^3 + \nu - \nu i_2 + \mu i_3 \tag{54}$$

where ν and μ are material constants, with $\mu \leq -8\nu/5$. In particular let us consider a matrix material that is given by eqn.(54), and ν =1, μ =-4.

Alternatively, the simplest model for the porous material can be obtained from the described scheme in Fig. 1 by selecting $N_\alpha = 2, N_\beta = 2, N_\gamma = 2$ subcells in the repeating cell. In this configuration the pore is represented by a single subcell ($\alpha = 1, \beta = 1, \gamma = 1$), while the remaining seven subcells are comprised of the nonlinear matrix. The volume fraction of the voids is therefore given by

$$v_f = \frac{d_1 h_1 l_1}{(d_1 + d_2)(h_1 + h_2)(l_1 + l_2)}$$

By choosing $d_1 = h_1 = l_1$ and $d_2 = h_2 = l_2$ a cubic equation is obtained for the relative dimension d_1/d_2 in terms of the porosity v_f. The resulting **GMC** response of the porous material can then be compared to the closed-form solution obtained using the spherical model.

Fig. 2(b) illustrates this comparison between the response to hydrostatic loading as predicted by the present micromechanical model (solid line) and that provided by the spherical model (dashed

line). The figure shows the response for three volume fractions of porosities (or voids) namely v_f = 0.1, 0.3, 0.5. Also included in the figure and denoted by the label $v_f = 0$, is the response of the pure harmonic material itself. It can be clearly seen that the correspondence between the two predictions is excellent in the small deformation regime and remains quite satisfactory as the deformation increases. Furthermore, the comparison improves as the volume fraction is increased. It should be noted, that in the framework of **GMC**, the pores are assumed to be arranged periodically in the composite; whereas in the spherical model a gradation of pores of various sizes is assumed, while maintaining the volume ratio A^3/B^3. This difference in pore geometry idealization is believed to be a primary factor behind any discrepancies between the two model predictions.

4.1.2 Class II

In this class of nonlinearly elastic compressible materials, the strain energy function is given by

$$W = c_1(i_1 - 3) + g(i_2) + c_3(i_3 - 1), \quad g''(i_2) \neq 0 \tag{55}$$

where g is an arbitrary function of the *second* invariant and c_i are material constants. Given this class the solution of eqn.(49) is given by

$$r(R) = [\xi R^2 + \frac{\eta}{R}]^{1/2} \tag{56}$$

Again, by imposing the boundary conditions given in eqns. (50), the constants ξ and η can be determined, and the average radial stress derived.

Following Murphy (1993), let us consider the following strain energy function:

$$W = \frac{1}{8}(\bar{\lambda} + 2\mu){i_2}^2 + \frac{1}{4}(2\mu - 3\bar{\lambda})i_2 - 4\mu(i_3 - 1) + \frac{9}{8}\bar{\lambda} - \frac{15}{4}\mu \tag{57}$$

Here $\bar{\lambda}$ and μ are the Lame' constants of the material, with the specific values for the material employed here being $\bar{\lambda}$ =2 and μ =1.

Fig. 2(c) presents comparisons between the response to hydrostatic loading as predicted by **GMC** and that provided by the spherical model for three volume fractions of porosities namely v_f = 0.1, 0.3, 0.5. Also included in the figure is the response of the pure matrix material denoted by the label $v_f = 0$. Once again, good correspondence between the two model predictions are observed, with very good agreement occurring for volume fractions exceeding 0.3.

4.1.3 Class III - Generalized Varga Material

Here the strain energy function for this class of materials is defined by

$$W = c_1(i_1 - 3) + c_2(i_2 - 3) + h(i_3), \quad h''(i_3) \neq 0 \tag{58}$$

where h is an arbitrary function of the *third* invariant and c_i are again material constants. In this case the solution of eqn.(49) is given by

$$r(R) = [\xi R^3 + \eta]^{1/3} \tag{59}$$

and once again, imposing the boundary conditions in eqns.(50), the constants ξ and η can be determined, and the average radial stress derived.

For this class we will consider the following strain energy function discussed in Haughton(1987):

$$W = 2\mu[i_1 - 3 - \frac{1 - i_3^{-p}}{p}] \tag{60}$$

Here μ is the shear modulus of the material, and p is a parameter such that $p > -1/3$. The specific material parameters used here are μ =1 and $p = -0.1$.

In keeping with previous discussions, comparisons between the response of the porous material to hydrostatic loading as predicted by **GMC** and the spherical mode are now shown in Fig. 2(d) for same three volume fractions of porosities, i.e., v_f = 0.1, 0.3, 0.5. Also, as done previously the response of the generalized Varga material to hydrostatic loading (labeled by $v_f = 0$) is included to validate the particular constitutive model implementation. Clearly, the correspondence between the predictions of the two models is once again satisfactory, however, for this class the comparison has deteriorated relative to the other two classes of materials.

Finally, the comparisons between **GMC** and the spherical model predictions shown in Fig.(2) indicate the reliability of the present micromechanical model for this type of loading. Also, it has been shown that the validity of the predicted response is not significantly affected by the type of chosen nonlinear material, although for some classes of materials the agreement between the two methods appears slightly better than for others. This variation in agreement may be attributed to 1) the fact that in the spherical model each class of material produces its own unique spatial dependence for the three invariants i_1, i_2, and i_3 (see equations (53),(56) and (59)) or 2) to the need for additional refinement in the GMC - RVE so as to better approximate the spherical nature of the void, which is presently represented as a cube, and thus better capture the spatial dependence. Further investigation of these factors will be reserved for future work.

As a final comment relative to the validation of the implementation of **GMC**, it should mentioned that by taking all subcells to be of the same material, the obtained response from **GMC** coincides with that of the monolithic material model itself. This is of course a necessary condition that **GMC** must and does satisfy in all cases considered in this section as well as in the next sections.

4.2 Results

4.2.1 Discontinuous Reinforced Composites

Let us consider a nonlinearly elastic particulate composite that consists of an aluminum alloy 8091 reinforced by S_iC particles. Both materials are considered to be nonlinearly elastic and described by Murnaghan's representation (see Table 1). The elastic moduli of the S_iC particles and the elastic constants of the aluminum alloy Al 8091 matrix were taken from Chen and Jiang (1993) and are shown in Table 2.

Table2: Material constants for SiC/Al 8091 system

Constituents	Material Constants (GPa)				
	λ	μ	l	m	n
SiC	97.66	188	−82.1	−310	−683
Al 8091	44.93	31	−218	−378	−435

In Fig. 3 the response of the resulting strongly bonded particulate composite is shown under uniaxial stretching (that is, with $\bar{F}_{11} = \bar{\lambda}_1$ being prescribed, while $\bar{F}_{22} = \bar{\lambda}_2 = 1$ and $\bar{F}_{33} = \bar{\lambda}_3 = 1$) . Here both the response in tension and compression for two volume fractions of reinforcement, namely $v_f = 0.3$ and 0.5, and the corresponding response of the **unreinforced** nonlinear aluminum matrix (labeled as $v_f = 0$) are shown. The figure clearly exhibits the overall nonlinear behavior of the composite and the significant stiffening influence that increasing the volume fraction of reinforcement would have. It should be noted that under tensile stretching, the matrix (i.e., $v_f = 0$) exhibits at a certain stage of loading (i.e., $\bar{\lambda}_2 \approx 1.05$) an instability in the sense that the stress-deformation curve starts to decrease. All computed responses in Fig. 3 have been stopped at this stage of loading. Note, as one might expect, with increasing reinforcement volume fraction, the composite deformation at which matrix instability sets in is decreased.

4.2.2 Continuous Reinforced Composites

Next consider a continuous fiber reinforced S_iC/Al composite system with a fiber volume fraction of 0.4. The material constants are again as specified in Table 2. The response of the continuously reinforced system is shown in Fig. 4 given an applied uniaxial stress loading in the fiber direction (1-direction, Fig. 4(a)) and in the transverse direction (2 -direction, Fig. 4(b)). Also included in Fig. 4 are the response of the constituents, that is the fiber material, denoted by $v_f = 1$, Fig. 4a, (which is seen to be quite linear in the chosen range of deformation) and the highly nonlinear unreinforced Al- matrix, denoted by $v_f = 0$ in Fig. 4(b). Figure 4 clearly exhibits the nonlinearity and directionality effects of the fibrous composite, for instance note the six fold increase in longitudinal load carrying capacity relative to that in the transverse direction. Similarly, comparing Figs. 3 and 4 one immediately sees the advantage of continuous reinforcement scenarios.

Now assuming that the ultimate strain of the S_iC fiber is identical to that of the ceramic SCS-6 fiber, namely 0.01 and following the evolution of the elastic fields in the fiber and matrix subcells, it turns out that for the longitudinal loading case (loading in the fiber direction) the fiber will break well within the linear axial stress-stretch region shown in Fig. 4(a). In this case the average stretch $\bar{\lambda}_1$ is also equal to 1.01. Alternatively, in the case of transverse loading, fiber breakage does not take place in the tensile portion (which is highly nonlinear) of the stress-stretch response shown in Fig. 4(b). Nevertheless, just at the final point of the graph the local stretch in the matrix reaches the value 1.0584 which is high. Thus it may be accurate to assume that the matrix phase will fail before reaching the final value of the tensile portion of the transverse response shown in Fig. 4b.For the transverse compressive response, fiber breakage occurs when the stretch in the matrix is rather high (e.g. 0.963), namely within the nonlinear region. The average stretch $\bar{\lambda}_2$ was 0.98. These results indicate that for transverse loading, nonlinearity effects do indeed influence the response of the composite before its failure and thus cannot be ignored. As a final remark, it is important to remember that the significance of incorporating nonlinearity effects into the deformation and life analysis of composites becomes even more critical in the presence of weak interfaces, since the local stress and strain states around an inclusion are increased greatly due to the "opening-up" of such a weak interfaces.

4.2.3 Cellular Materials

It is well known that in cellular solids or foams the cells are either closed or open (Gibson and Ashby,1988). An idealized structure of an open-cell foam is shown in Fig. 5(a), where the solid material is distributed in little columns or beams which form the cell edges (as opposed to the closed-cell case where the solid material is distributed in little plates which form the faces of the cells). The nonlinear response of closed-cell foams can be modeled straight forwardly using **GMC** by simply choosing the void as a single subcell surrounded by solid matrix material. Just such a geometrical model was employed to predict the porous material responses shown in Fig. 2. It is also, however, quite possible to model open-cell foams using GMC as well, and obtain their nonlinear elastic response. To this end, referring to Figs. 1 and 5(b), consider a repeating cell with $N_\alpha = 2,\ N_\beta = 2,\ N_\gamma = 2$ subcells. Now filling subcells (α,β,γ)= (1,1,1), (1,2,1), (1,2,2) and (2,2,1) with solid material and considering the remaining subcells (1,1,2), (2,1,1), (2,1,2) and (2,2,2) to be comprised of voids, one can immediately obtain a repeating cell that idealizes open-cell foams.

The volume fraction of voids in these open-cells structure is given by

$$v_f = \frac{d_1 h_1 l_2 + d_2 h_1 l_1 + d_2 h_1 l_2 + d_2 h_2 l_2}{(d_1 + d_2)(h_1 + h_2)(l_1 + l_2)}$$

By choosing $d_1 = h_2 = l_1$ and $d_2 = h_1 = l_2$, one obtains a cubic equation for the relative dimension d_1/d_2. Thus the latter can be determined for a given amount of porosity v_f.

It was shown by Gibson and Ashby (1988) that an open-cell approach approximates the Young's modulus of polymer foams quite well. This was accomplished using an expression based on mechanics (or a strength) of materials approach which takes explicitly into account the bending of the open-cell walls caused by loading. Alternatively, **GMC** is a continuum based formulation and consequently bending of the individual subcells is not directly accounted for, thereby potentially restricting the maximum volume content of voids realizable. A comparison of the Gibson and Ashby formula with **GMC** predictions based on the idealization shown in Fig. 5, verifies that the prediction of Young's modulus for porous materials are in agreement with each other for foam porosities in the range of $0 \leq v_f \leq 0.6$. For higher porosities the individual ligament aspect ratios become such that the effect of bending on the cell walls is significant and must be accounted for. Consequently, the modeling of open celled foams using **GMC** in compression is expected to be valid for only lower volume fractions of porosities.

GMC predictions for the response of both an open- and closed-cell foam, subjected to a uniaxial

stress loading (in the 1-direction), is illustrated in Fig. 6. The solid matrix is represented by the strain energy function attributed to Blatz (1969) in Table 1. For a polyurethane rubber, the material constants are (Blatz and Ko, 1962): $\mu = 0.234MPa$, $K = 3.27GPa$, and $k = 13.3$. The figure shows both the average uniaxial stress and average uniaxial lateral contraction versus the longitudinal extension ratio of the foam rubber, given a 0.47 volume fraction of voids. Clearly, the open-cell foam exhibits a weaker stiffness (or "softer" overall response) as compared to the closed-cell case. Although this is expected, the figure illustrates the capability of **GMC** to predict the nonlinear response of both types of porous materials.

5 Conclusions

The generalized method of cells (**GMC**) micromechanics methodology has been extended to predict the finite deformation behavior of nonlinear thermoelastic composites. The micromechanical analysis relies on the tangential formulation of each phase of the composite (according to which the stress increment is expressed in terms of the deformation gradient increment via the instantaneous tangent tensor of the constituent material). This tangential formulation has been shown to possess two significant advantages over the previously used secant approach, in that 1) the instantaneous concentration tensors of the composite as well as its current effective tangent tensors can be established and 2) at every increment of loading only a system of linear algebraic equations needs to be solved. Verification of this nonlinearly elastic **GMC** micromechanics model was accomplished by comparing the response of three classes of porous materials with those obtained from an analytical spherical model (whose prediction is valid for hydrostatic loading only). Good agreement between the analytical spherical model and **GMC** was shown for all three classes of materials given various amounts of porosities. Similarly, the response of nonlinearly elastic particulate and continuous fiber reinforced S_iC/Al composite systems were calculated and discussed. Results clearly exhibit the effects of the nonlinearity of the phases and strongly suggest the need for such a finite deformation micromechanics model as described herein; particularly when one is interested in predicting failure of such composite systems. Finally the capability of **GMC** to predict the nonlinear response of opened- and closed-cell cellular solids was demonstrated.

With an eye toward the future, having established the effective behavior of the composite at any stage of loading, it is now possible to proceed and predict the behavior of nonlinearly elastic laminated materials. To this end, we propose to utilize the analysis of laminated flexible composites

under finite deformation as presented by Chou(1992). This can be achieved by solely using the nonlinear properties of the isotropic constituents of the composite in conjunction with the present micromechanical analysis, without the need to employ a strain energy function that describes a nonlinearly elastic anisotropic material. The definition of such a strain energy function naturally involves numerous parameters, the determination of which might be very complicated. Similarly, equations of state for thermoelastic rubber-like solids were recently discussed by Ogden(1992) and can be implemented into the present methodology for the prediction of the thermoelastic response of reinforced rubber-like solids which are capable of undergoing finite deformation.

6 Acknowledgment

The first author gratefully acknowledges the support of the Diane and Arthur Belfer chair of Mechanics and Biomechanics and the NASA Lewis Research Center under NAG 3-1377.

References

Aboudi, J. (1986) Overall finite deformation of elastic and elastoplastic composites. Mech. Materials. **5**, 73-86.

Aboudi, J. (1989) Micromechanical analysis of composites by the method of cells. Appl. Mech. Rev. **42**, 193-221.

Aboudi, J. (1991) Mechanics of Composite Materials: A Unified Micromechanical Approach. Elsevier, Amsterdam.

Aboudi, J. (1995) Micromechanical analysis of thermoinelastic multiphase short-fiber composites. Composites Eng. **5**, 839-850.

Aboudi, J. (1996) Micromechanical analysis of composites by the method of cells - Update. Appl. Mech. Rev. **49**, S83-S91.

Bland, D.R. (1969) Nonlinear dynamic elasticity. Blaisdell, Waltham.

Blatz, P.J. (1969) Application of large deformation theory to the thermomechanical behavior of rubberlike polymers- porous, unfilled, and filled. In: Rheology - Theory and Applications, vol. **5**, (ed. F.R. Eirich), pp.1-55. Academic Press, New York.

Blatz, P.J. and Ko, W.L. (1962) Application of finite elastic theory to the deformation of rubbery materials. Trans. Soc. Rheology **6**, 223-251.

Chen, Y.C. and Jiang, X. (1993) Nonlinear elastic composites of particulate composites. J. Mech. Phys. Solids **41**, 1177-1190.

Chou, T-W (1992) Microstructural Design of Fiber Composites. Cambridge University Press, Cambridge.

Gibson, L.J. and Ashby, M.F. (1988) Cellular Solids. Pergamon, Oxford.

Hashin, Z. (1985) Large isotropic elastic deformation of composites and porous media. Int. J. Solids Structures **21**, 711-720.

Herakovich, C.T. (1997) Mechanics of Fibrous Composites. Wiley, New York.

Haughton, D.M. (1987) Inflation and bifurcation of thick-walled compressible elastic spherical shells. IMA J. Appl. Math **39**, 259-272.

Horgan, C.O. (1995) On axisymmetric solutions for compressible nonlinearly elastic solids. Z. angew Math. Phys. **46**, S107-S125.

Iman, A., Johnson, G.C., and Ferrari, M. (1995) Determination of the overall moduli in second order incompressible elasticity. J. Mech. Phys. Solids **43**, 1087-1104.

Murnaghan, F.D. (1967) Finite Deformation of an Elastic Solid. Dover, New York.

Murphy, G.J. (1993) Inflation and eversion of spherical shells of a special compressible material. J. Elasticity **30**, 251-276.

Ogden, R.W. (1974) On the overall moduli of non-linear elastic composite materials. J. Mech. Phys. Solids. **22**, 541-553.

Ogden, R.W. (1984) Non-Linear Elastic Deformations. Ellis Horwood, Chichester, England.

Ogden, R.W. (1992) On the thermoelastic modeling of rubberlike solids. J. Thermal Stresses **15**, 533-557.

Ponte Castaneda, P. and Willis, J.R. (1988) On the overall properties of nonlinearly viscous composites. Proc. Roy. Soc. London A **416**, 217-244.

Sussman, T. and Bathe, K.J. (1987) A finite element formulation for nonlinear incompressible elastic and inelastic analysis. Computers & Structures **26**, 357-409.

Talbot, D.R.S. and Willis, J.R. (1987) Bounds and self-consistent estimates for the overall properties of nonlinear composites. IMA J. Appl. Math. **39**, 215-240.

Willis, J.R. (1990) Variational estimates for the overall behavior of a nonlinear matrix-inclusion composite. In: Micromechanics and Inhomogeneity (ed. G.J. Weng, M.Taya and H. Abe), 581-597, Springer- Verlag, New York.

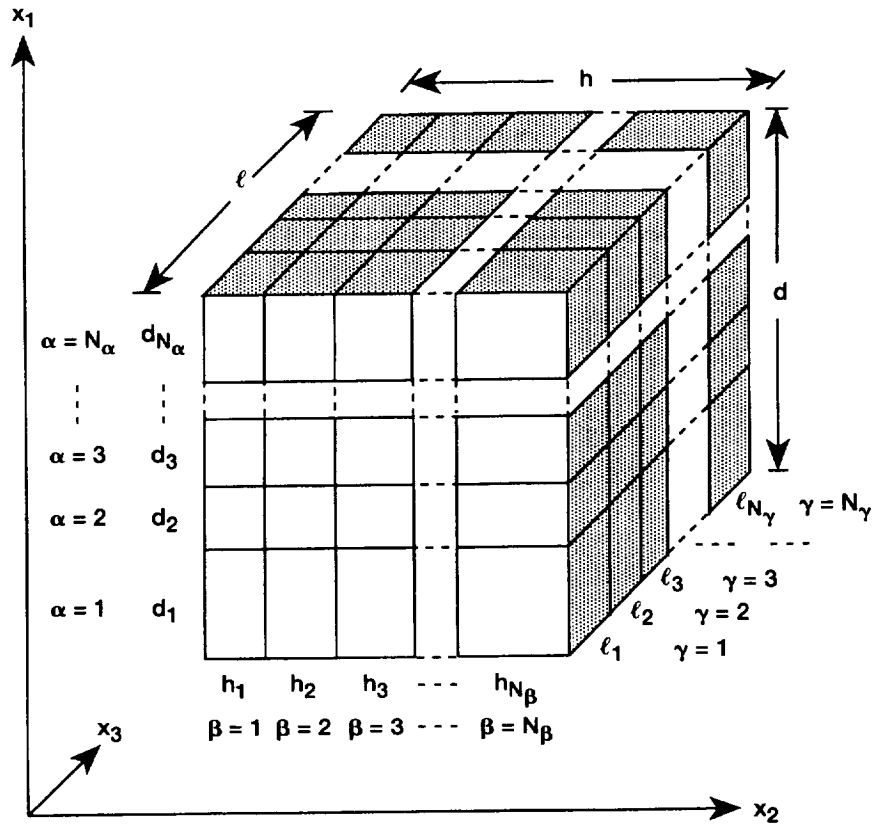

Figure 1.—A repeating cell in GMC consisting of N_α, N_β and N_γ subcells in the 1, 2 and 3 directions, respectively.

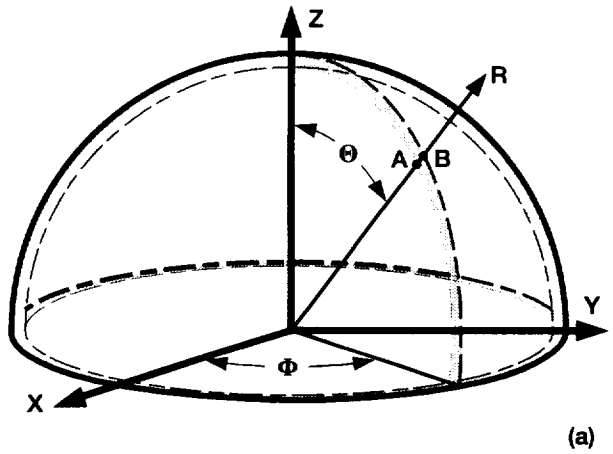

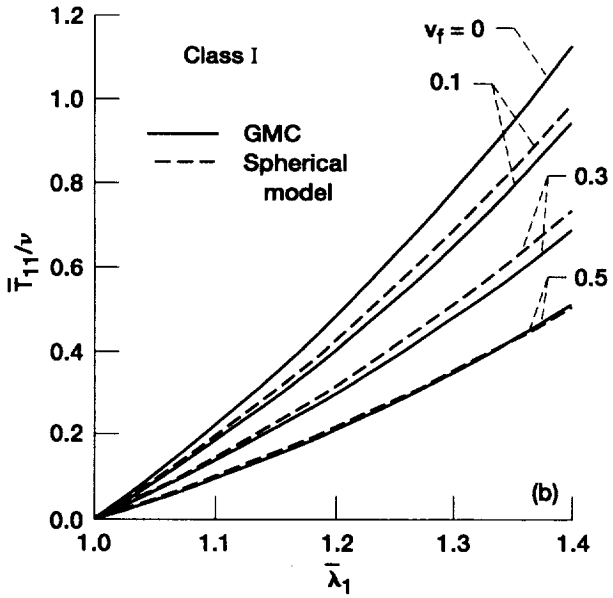

Figure 2.—Comparisons between GMC and the spherical model prediction for three types of nonlinearly elastic porous materials under a hydrostatic loading. (a) Shell geometry. (b) Class I (harmonic material). (c) Class II. (d) Class III (generalized Varga material).

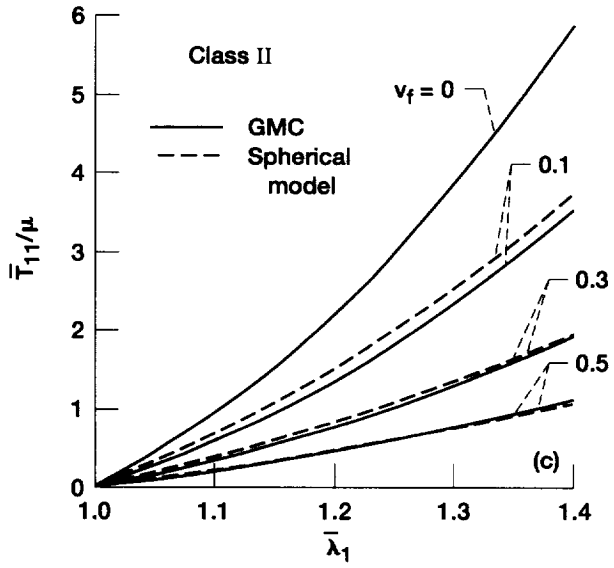

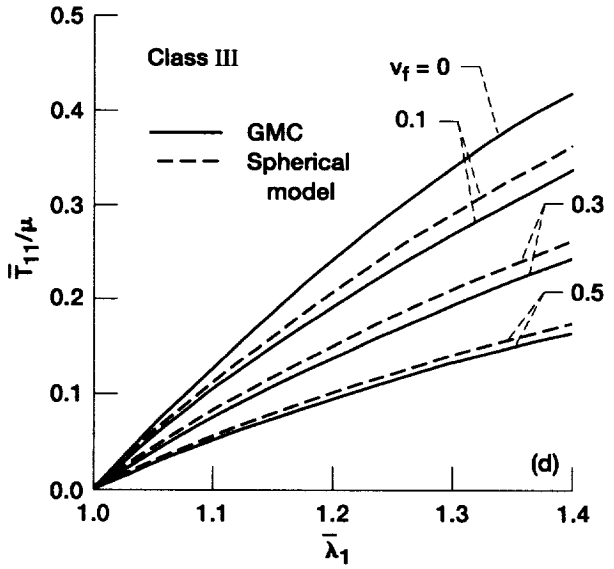

Figure 2.—Concluded. (c) Class II. (d) Class III (generalized Varga material).

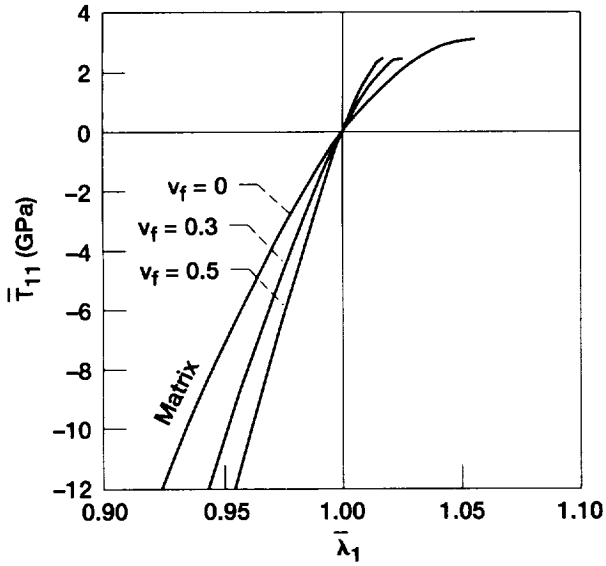

Figure 3.—The response of nonlinearly elastic particulate composite (SiC/Al) subjected to uniaxial stretching.

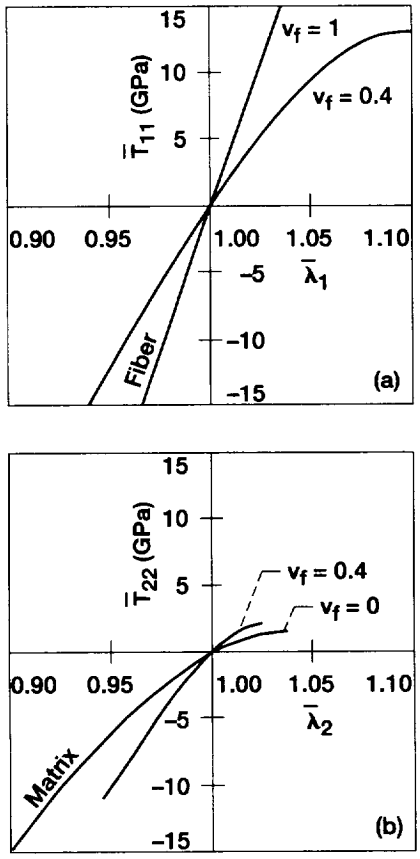

Figure 4.—The response of a nonlinearly elastic long-fiber composite (SiC/Al) subjected to uniaxial stress loading. (a) Loading in the fiber 1-direction. (b) Loading in the traverse 2-direction.

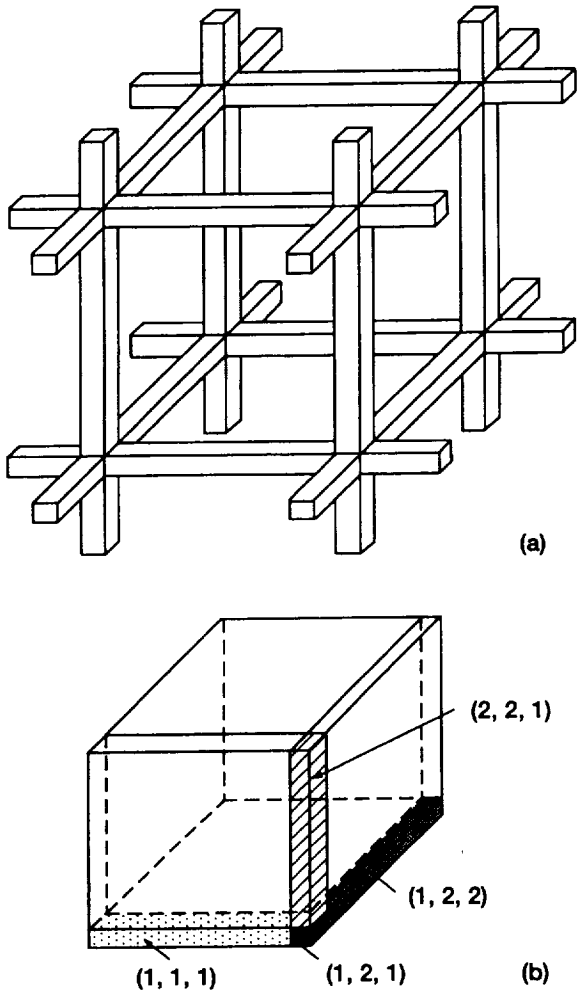

Figure 5.—An idealized three-dimensional structure of open-cell foams (a). The corresponding repeating cell for the modeling of the open-cells structure by GMC (b).

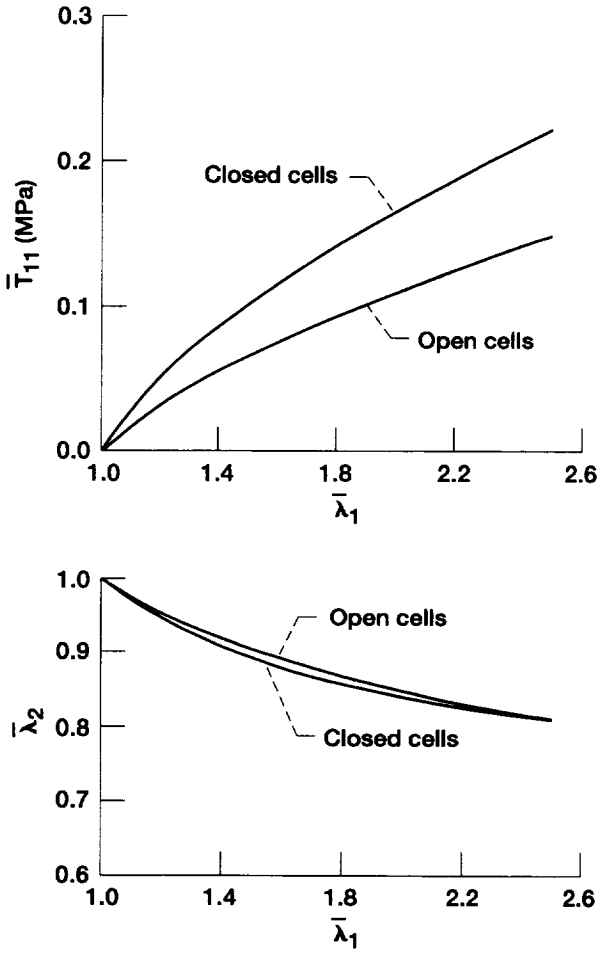

Figure 6.—Average uniaxial stress and average uniaxial lateral contraction versus average longitudinal extension ratio of a porous polyurethane rubber modeled as closed and open-cells cellular solid.

REPORT DOCUMENTATION PAGE

Form Approved
OMB No. 0704-0188

1. AGENCY USE ONLY (*Leave blank*)	2. REPORT DATE	3. REPORT TYPE AND DATES COVERED
	July 1997	Technical Memorandum

4. TITLE AND SUBTITLE

Micromechanical Modeling of the Finite Deformation of Thermoelastic Multiphase Composites

5. FUNDING NUMBERS

WU-523-31-13-00

6. AUTHOR(S)

Jacob Aboudi and Steven M. Arnold

7. PERFORMING ORGANIZATION NAME(S) AND ADDRESS(ES)

National Aeronautics and Space Administration
Lewis Research Center
Cleveland, Ohio 44135-3191

8. PERFORMING ORGANIZATION REPORT NUMBER

E-10843

9. SPONSORING/MONITORING AGENCY NAME(S) AND ADDRESS(ES)

National Aeronautics and Space Administration
Washington, DC 20546-0001

10. SPONSORING/MONITORING AGENCY REPORT NUMBER

NASA TM-107531

11. SUPPLEMENTARY NOTES

Jacob Aboudi, Faculty of Engineering, Tel-Aviv University, Ramat-Aviv 69978, Israel and Steven M. Arnold, NASA Lewis Research Center. Responsible person, Steven M. Arnold, organization code 5920, (216) 433-3334.

12a. DISTRIBUTION/AVAILABILITY STATEMENT

Unclassified - Unlimited
Subject Category 24

This publication is available from the NASA Center for AeroSpace Information, (301) 621-0390.

12b. DISTRIBUTION CODE

13. ABSTRACT ***(Maximum 200 words)***

A micromechanical model is proposed for the prediction of nonlinearly thermoelastic, multiphase particulate and/or continuous reinforced composites in which any or all constituents exhibit large strain (finite deformation). The analysis provides closed-form representations for the instantaneous mechanical and thermal concentration tensors as well as the effective tangent mechanical and thermal properties of the composite. The micromechanical model predictions are assessed by a comparison with an analytical spherical composite model, valid for hydrostatic loadings only. Very good agreement between the two approaches were obtained. Similarly, results demonstrating the effects of nonlinearity are given for particulate and continuous fiber reinforced $S_i C/Al$ composites. Finally, the nonlinear response of cellular solids idealized by open-cell and closed-cell structures are compared and contrasted.

14. SUBJECT TERMS	15. NUMBER OF PAGES
Micromechanics; Thermoelastic; Finite deformation; Nonlinear material; Incompressible material	30
	16. PRICE CODE: A03

17. SECURITY CLASSIFICATION OF REPORT	18. SECURITY CLASSIFICATION OF THIS PAGE	19. SECURITY CLASSIFICATION OF ABSTRACT	20. LIMITATION OF ABSTRACT
Unclassified	Unclassified	Unclassified	